Advanced Physical Research
Vol.7, No.2, 2025, pp.240-247
https://doi.org/10.62476/apr.72240

LOCALIZED PLASMON-POLARITONS IN MULTILAYER MAGNETOELECTRIC HYPERBOLIC METAMATERIALS

Nguyen Pham Quynh Anh*

Faculty of Engineering and Technology, Saigon University, Ho Chi Minh City, Vietnam

Abstract. An effective method for evaluating both transverse and longitudinal permeability in multilayer metal-dielectric hyperbolic metamaterials is presented. These permeability values, combined with known permittivity components, are used to determine the conditions required for the excitation of localized plasmon-polaritons under both TE and TM polarizations. The influence of structural parameters and external factors on plasmon-polariton excitation is thoroughly examined. It is shown that TE-polarized plasmon-polaritons can only be excited under specific conditions, such as when a sufficiently high number of layers is used, and the incident angle exceeds 55^0. In contrast, TM-polarized plasmon-polaritons are found to exhibit broader excitation conditions, with multiple configurations and a wider range of wavelengths supporting their formation. These findings reveal that TM-polarized modes are more flexible, whereas TE-polarized modes require stricter structural and angular constraints. The importance of accurate permeability evaluation in predicting and controlling plasmonic behavior in these materials is emphasized, as even small changes in structural design or external conditions can strongly impact the excitation of plasmon-polaritons. These insights contribute to a deeper understanding of how structural and environmental factors affect plasmon-polariton behavior, providing a foundation for future advancements in metamaterials and plasmonic technologies.

Keywords: plasmon-polariton, metamaterials, magnetoelectric hyperbolic metamaterials, permeability, metal-dielectric structures.

***Corresponding author:** Nguyen Pham Quynh Anh, Nguyen Pham Quynh Anh, aFaculty of Engineering and Technology, Saigon University, 273 An Duong Vuong Street, Ward 2, District 5, Ho Chi Minh City, Vietnam, e-mail: *npqanh@sgu.edu.vn*

Received: 23 February 2025; Revised: 28 April 2025; Accepted: 12 May 2025; Published: 24 June 2025.

1 Introduction

The interaction between electromagnetic radiation and hyperbolic metamaterials (HMMs) has attracted considerable attention in recent years, owing to their transformative potential in manipulating light and enabling advanced imaging techniques (Lee et al., 2020; Slobozhanyuk et al., 2015; Nguyen et al., 2023; Wang et al., 2023). HMMs are defined as engineered structures characterized by hyperbolic dispersion, which allows for the realization of unique optical properties. These materials are typically described using a uniaxial dielectric permittivity tensor with principal components that possess opposite signs, while the magnetic permeability is often approximated as unity (Kurilkina et al., 2016; Noginov et al., 2009; Li et al., 2016; Kanungo et al., 2010; Wurtz et al., 2011).

However, the behavior of electromagnetic waves in these materials is fundamentally influenced by both the dielectric permittivity and the magnetic permeability. The interplay between these parameters significantly affects the dispersion characteristics of the waves. Specifically, the dielectric response plays a crucial role in the behavior of TM-polarized waves, while the magnetic response becomes essential for TE-polarized waves, particularly in structures with engineered magnetic properties (Sun et al., 2014; Chettiar et al., 2006; Amiri, 2020; Sun et al., 2014).

Recent advances have highlighted the potential for artificially inducing magnetism in metamaterials, leading to the development of various magnetic metamaterials, including designs featuring metallic strips, split-ring resonators, and mesh configurations. Notably, magnetoelectric hyperbolic metamaterials, derived from multilayer metal-dielectric systems, have emerged as a promising avenue for enhancing the manipulation of electromagnetic waves (Kolmychek et al., 2018; Novikov, 2020; Carvalho et al., 2024; Song et.al, 2020).

A key aspect of these materials is the generation of surface plasmon-polaritons (PPs), particularly at the interface of media with opposing dielectric properties. The excitation of PPs can be utilized for various applications, including enhanced imaging resolution and increased control over light-matter interactions (Zayats et al., 2005; Wang et.al, 2019; Ahmad et al., 2024). This study aims to investigate the conditions for generating localized plasmon-polaritons at the boundaries of magnetoelectric hyperbolic metamaterials, focusing on the effects of structural parameters and polarization on excitation mechanisms. Through this analysis, new insights into the manipulation of electromagnetic waves in HMMs can be achieved, paving the way for innovative applications in photonics and nanotechnology.

2 Material parameters of planar metamaterial consisting of alternating layers of metal and dielectric

Let us consider the interface between two media: an isotropic dielectric with permittivity ε_1 and magnetic permeability $m_1 = 1$ and a magnetoelectric hyperbolic metamaterial (MEHMM). Let us assume that the optical axis of the MEHMM is orthogonal to the interface and collinear to the Z axis of the selected coordinate system. In the effective medium approximation, the MEHMM is considered as a uniaxial medium whose dielectric and magnetic properties are described by permittivity and magnetic permeability tensors, respectively:

$$\hat{e}_2 = \begin{pmatrix} e_0 & 0 & 0 \\ 0 & e_0 & 0 \\ 0 & 0 & e_e \end{pmatrix}, \ \hat{\mu}_2 = \begin{pmatrix} \mu_0 & 0 & 0 \\ 0 & \mu_0 & 0 \\ 0 & 0 & \mu_e \end{pmatrix}, \tag{1}$$

where e_o and e_e are the transverse (along the X, Y axes in the plane of the interface) and longitudinal (along the Z axis) principal permittivities, determined by the expressions (Shekhar et al., 2014)

$$e_o = fe_m + (1-f)e_d, e_e = \frac{e_m e_d}{fe_d + (1-f)e_m}, \tag{2}$$

where ee_m and e_d are the permittivities of the metal and the dielectric, f is the filling factor (the volume fraction of the metal in the nanostructure).

Using the transfer matrix method for layered media, we calculate the complex reflection and transmission coefficients for angles of incidence from 0° to 90° for TE and TM polarization (Shekhar et al., 2014). This program gives results for the amplitude transmission coefficients of s (TE)- and p (TM)-polarized waves (modules of these coefficients and their phases). Let's take the phase for the case of normal incidence and divide by the thickness of the structure, we get $k_{z2}(\theta_{in} = 0)$. As can be seen from the article (Rakic et al., 1998), for the case of normal incidence, we have:

$$k_0^2 e_o \mu_o = k_{z2}^2(\theta_{in} = 0), k_0 = \frac{2\pi}{\lambda}. \tag{3}$$

Considering that

$$e_o = Ree_o + iIme_o, \ e_e = Ree_e + iIme_e,$$

$$\mu_o = Re\mu_o + iIm\mu_o, \mu_e = Re\mu_e + iIm\mu_e, \tag{4}$$

and substituting (4) into (3) we get a system of two equations with two unknowns $Re\mu_o$ and $Im\mu_o$. Solving them in the usual way, we can determine these unknown quantities.

$$\mathrm{Re}\mu_0 = \frac{k_z^2 \mathrm{Ree}_0}{k_0^2\left(\mathrm{Ime}_0^2 + \mathrm{Ree}_0^2\right)},$$

$$\mathrm{Im}\mu_0 = \frac{-k_z^2 \mathrm{Ime}_0}{k_0^2\left(\mathrm{Ime}_0^2 + \mathrm{Ree}_0^2\right)}. \tag{5}$$

From (Rakic et al., 1998) we get the dispersion equation for TE-polarized wave in the following form

$$\frac{k_0^2 \sin^2\theta_{in}(Re\mu_o + iIm\mu_o)}{Re\mu_e + iIm\mu_e} + k_z^2(\theta_{in} \neq 0) = k_0^2(Ree_o + iIme_o)(Re\mu_o + iIm\mu_o). \tag{6}$$

By equating the real and imaginary parts of the expression on the left and right, from (6) we can find: $Re\mu_e$ and $Im\mu_e$

$$Re\mu_e = \frac{k_0^2 \sin^2\theta\left(-AIm\mu_o + k_0^2\cos^2\theta Re\mu_o - BRe\mu_o\right)}{M},$$

$$Im\mu_e = \frac{k_0^2 \sin^2\theta\left(k_0^2\sin^2\theta Im\mu_o + CIm\mu_o + DRe\mu_o\right)}{M}, \tag{7}$$

where

$$A = Im\mu_o Ree_o, B = Ree_o Re\mu_o,$$
$$C = Ime_o Im\mu_o, D = Ime_o Re\mu_o,$$
$$M = k_0^4\cos^4\theta + 2Ck_0^2\cos^2\theta + C^2 + A^2 - -2Bk_0^2\cos^2\theta + D^2 + (Re\mu_o)^2.$$

As an illustration of the obtained results, we consider a magnetoelectric metamaterial based on a nanostructure composed of alternating layers of Ag metal and SiO_2 dielectric, with permittivities e_m and e_d thicknesses d_m and d_d, respectively. The permittivity of silver is modeled using the modified Drude formula (Simmons & Potter, 2000), while the permittivity of silicon dioxide is described by the Sellmeier equation (Papadakis, 2015). Following the steps outlined above, Figs. 1-3 present the spectral dependencies of the real and imaginary parts of the transverse and longitudinal permittivity and permeability for the Ag/SiO_2 metal-dielectric layered structure under TE and TM wave incidence.

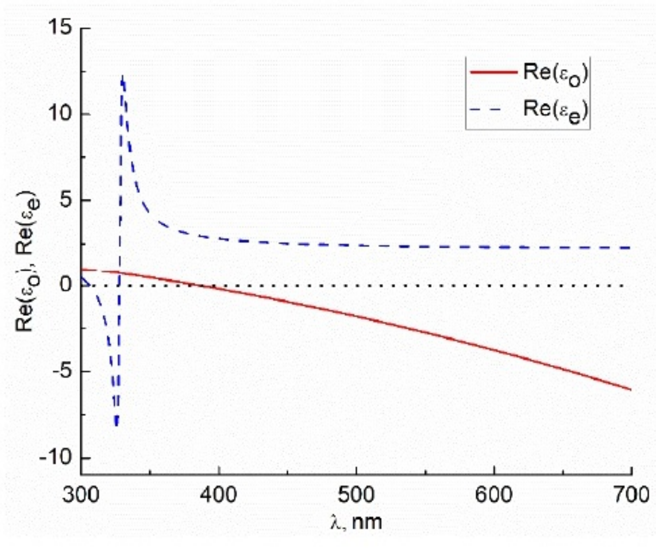

Figure 1: Spectral dependence of the real part of the transverse (solid curve) and longitudinal (dashed curve) permittivities of the multilayer Ag/SiO_2 structure with a filling factor of 0.333

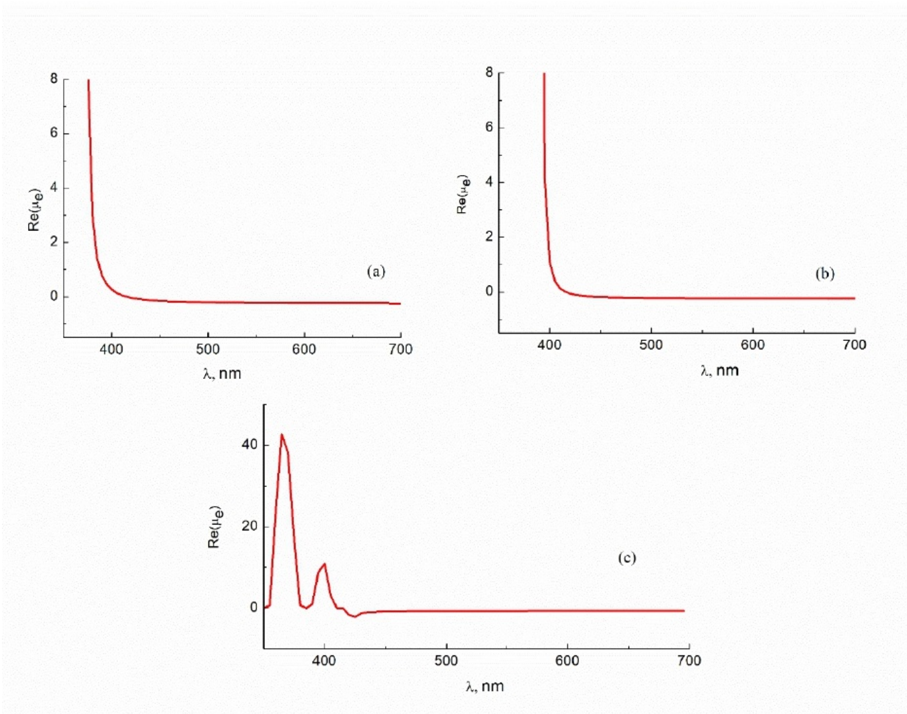

Figure 2: Spectral dependence of the real part of the transverse permeability of the Ag/SiO_2 structure consisting of (a) 5, (b) 7, (c) 21 layers for incident angle of 0 degree

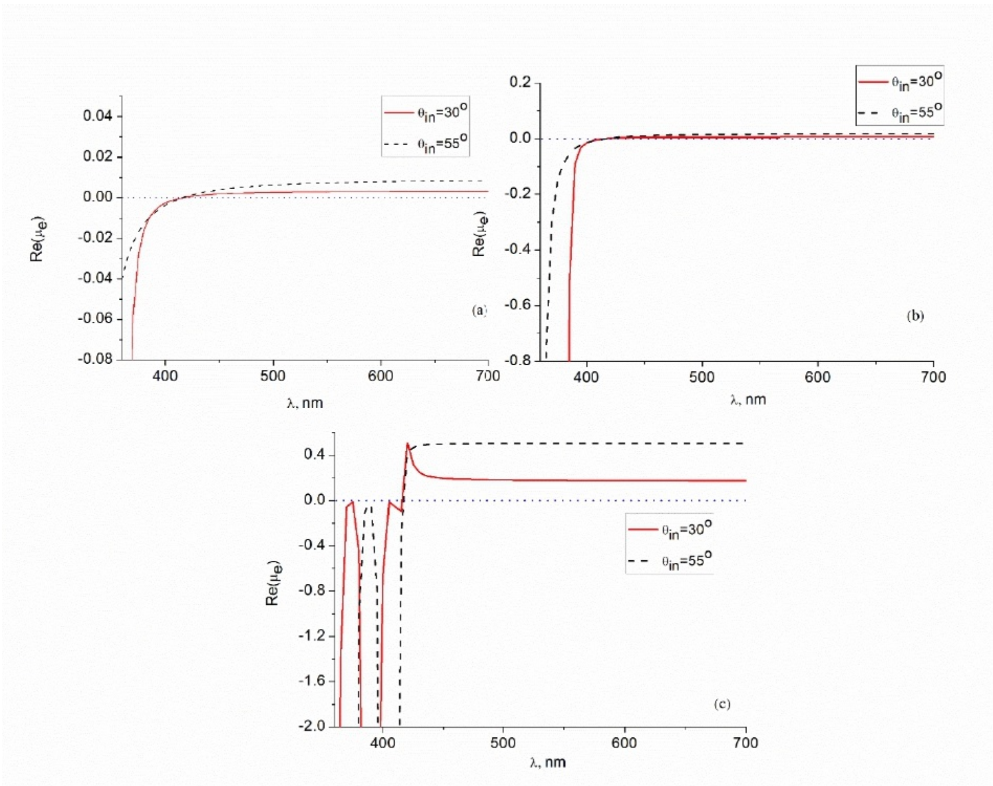

Figure 3: Spectral dependence of the real part of the longitudinal permeability of the Ag/SiO_2 structure consisting of (a) 5, (b) 7, (c) 21 layers for incident angle of 30 degrees (solid curve), 55 degrees (dashed curve). The filling factor is 0.333, the thickness of the silver layer is 20 nm

The calculations from Figs. 1-3 reveal that, within the spectral range of 390 - 415 nm, the wave vector surface for the TE-polarized wave takes the form of a two-sheeted hyperboloid. In this scenario, the metamaterial is classified as a Type II magnetoelectric hyperbolic metamaterial (MHMM II^{TE}). However, when $\lambda < 390\,nm$ or $\lambda > 415\,nm$, the wave vector surface transitions to a one-sheeted hyperboloid, and the metamaterial is identified as Type I magnetoelectric hyperbolic metamaterial (MHMM I^{TE}). For the TM-polarized wave, the metamaterial demonstrates Type II behavior (MHMM II^{TM}) within the same spectral range of 390 - 415 nm, while exhibiting Type I behavior (MHMM I^{TM}) under the condition $\lambda > 415\,nm$.

Fig. 3 indicates that changing the incident angle, for example, to 30 degrees or 55 degrees, alters the magnitude of the real part of the longitudinal permeability. However, the spectral range that excites hyperbolic metamaterial types remains unchanged.

3 Conditions for plasmon-polariton formation at the interface of dielectric medium and metal-dielectric multilayer metamaterials

Let a TE (TM)-polarized wave with wave vector be incident on the interface. The vectors of electric $\vec{E}$ and magnetic $\vec{H}$ intensity in the dielectric (1) and metamaterial (2) can be represented as

$$\vec{E}_1^{TE} = A_0^{TE}\vec{e}_y \exp[iq^{TE}x + \kappa_1^{TE}z], \overrightarrow{H}_2^{TE} = A_2^{TE}\left(i\frac{\kappa_1^{TE}}{k_0}\overrightarrow{e}_x + \frac{q^{TE}}{k_0}\overrightarrow{e}_z\right)\exp[iq^{TE}x + \kappa_1^{TE}z];$$

$$\vec{E}_2^{TE} = A_0^{TE}\vec{e}_y \exp[iq^{TE}x - \kappa_2^{TE}z], \overrightarrow{H}_2^{TE} = \frac{A_2^{TE}}{\mu_0}\left(-i\frac{\kappa_2^{TE}}{k_0}\overrightarrow{e}_x + \frac{q^{TE}}{k_0}\frac{\hat{A}\mu_0}{\mu_e}\overrightarrow{e}_z\right)\exp[iq^{TE}x - \kappa_2^{TE}z];$$

$$\overrightarrow{E}_1^{TE} = \frac{A_0^{TE}}{e_0}\left(i\frac{\kappa_1^{TE}}{k_0}\overrightarrow{e}_x + \frac{q^{TE}}{k_0}\overrightarrow{e}_z\right)\exp[iq^{TE}x + \kappa_1^{TE}z];$$

$$\vec{H}_1^{TM} = A_0^{TM}\vec{e}_y \exp[iq^{TM}x + \kappa_1^{TM}z]$$

$$\vec{E}_2^{TM} = \frac{A_0^{TM}}{\varepsilon_o}\left(i\frac{\kappa_2^{TM}}{k_0}\vec{e}_x - \frac{q^{TM}}{k_0}\frac{e_o}{e_e}\vec{e}_z\right)\exp[iq^{TM}x - \kappa_2^{TM}z],$$

$$\vec{H}_2^{TM} = A_0^{TM}\vec{e}_y \exp[iq^{TM}x - \kappa_2^{TM}z], \tag{8}$$

where $A_0^{TE,TM}$ is amplitude of TE- (TM-) polarized wave, $\kappa_{d,m}^{TE,TM}$ is damping constant, $q^{TE,TM}$ and $k_{z1,2}^{TE,TM}$ are, respectively, the transverse and longitudinal wave numbers (transverse and longitudinal components of the wave vector); $i.\kappa_{1,2}^{TE,TM} = k_{z1,2}^{TE,TM}$.

Considering Equation (8) and based on Maxwell's equations, the dispersion relations for TE- and TM-polarized waves in a dielectric and MGMM are derived as follows

$$(q^{\mathrm{TE,TM}})^2 + (k_{z1}^{\mathrm{TE,TM}})^2 = k_0^2\varepsilon_1, \tag{9}$$

$$(q^{\mathrm{TE}})^2\mu_o + (k_{z2}^{\mathrm{TE}})^2\mu_e = k_0^2\varepsilon_o\mu_o\mu_e, \tag{10}$$

$$(q^{\mathrm{TM}})^2\varepsilon_o + (k_{z2}^{\mathrm{TM}})^2\varepsilon_e = k_0^2\mu_o\varepsilon_o\varepsilon_e, \tag{11}$$

Calculations based on Equations (9), (10), and (11) demonstrate that TE-polarized localized surface plasmon-polaritons cannot exist in I^{TE} (I^{TM})-type MGMMs. For II^{TE} (II^{TM})-type MGMMs, the localization condition for plasmon-polaritons is given by

$$\varepsilon_o\mu_e > \varepsilon_1(\varepsilon_e\mu_o > \varepsilon_1) \tag{12}$$

Calculations (Figs. 1-3) performed for multilayer structures with 5, 7, and 21 layers show that TE-polarized localized plasmon-polaritons are only excited in Type II hyperbolic metamaterials consisting of alternating layers of Ag metal and SiO_2 dielectric when the structure contains 21 layers. In this case, excitation occurs within the wavelength range of 395–410 nm. For TM-polarized localized plasmon-polaritons, excitation is observed in Type II hyperbolic metamaterials across different configurations: in the 5-layer structure at wavelengths of 390–395 nm, in the 7-layer structure at 390–405 nm, and in the 21-layer structure at 390–407 nm. We observe that as the number of layers in the structure increases, the values of $Re\mu_o$ and $Re\mu_e$ also increase, simultaneously expanding the excitation spectral range. Additionally, an increase in the incident angle also broadens the range of values for λ.

Notably, TE-polarized plasmon-polaritons only appear in the 21-layer structure and when the incident angle exceeds 55°. Fig. 4 shows that as the incident angle increases from 55° to 90°, the excitation spectral range of the plasmon-polariton shifts towards shorter wavelengths, and its width also decreases. At 90°, TE-polarized localized plasmon-polaritons can no longer be excited in the examined structure.

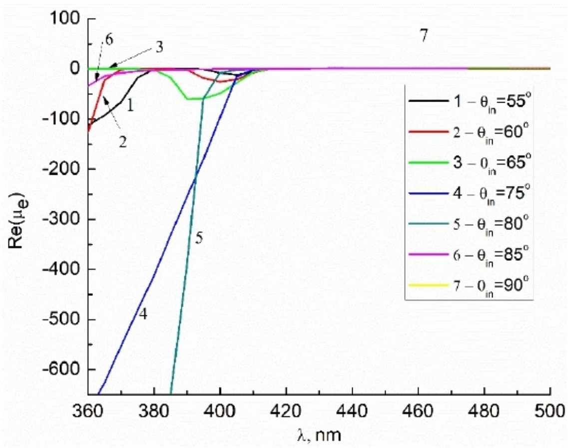

Figure 4: Spectral dependence of the real part of the longitudinal permeability of the multilayer Ag/SiO_2 structure consisting 21 layers for incident angle of 55° (curve 1), 60° (curve 2), 65° (curve 3), 75° (curve 4), 80° (curve 5), 85° (curve 6), 90° (curve 7). The filling factor is 0.333, the thickness of the silver layer is 20 nm

This demonstrates that the number of layers and the incident angle significantly impact the excitation of plasmon-polaritons in the multilayer metal-dielectric metamaterial structure. This finding was obtained by determining the permeability of the structure using a new approach - employing transfer matrix theory to extract the parameters of individual layers, rather than treating the entire structure as a homogeneous medium, as in the effective medium theory approach.

4 Conclusion

In this paper, we demonstrated that the use of phase determination via transfer matrix theory is an effective method for accurately calculating the wavevector component, which allows for the precise determination of both transverse and longitudinal permeability. With these permeability values, along with known permittivity components, we thoroughly assessed the conditions required for exciting localized plasmon-polaritons in both TE and TM polarizations. The findings reveal that TE-polarized localized plasmon-polaritons are only excited under specific conditions, such as a sufficiently high number of layers (e.g., 21 layers) and incident angles greater than 55°. In contrast, TM-polarized localized plasmon-polaritons exhibit broader excitation conditions across multiple configurations (e.g., 5, 7, and 21 layers) and over a wider wavelength range. These results highlight the strong influence of structural parameters (e.g., layer number) and external factors (e.g., incident angle) on the excitation of plasmon-polaritons, emphasizing the importance of precise permeability determination for predicting and controlling plasmonic behavior in multilayer metal-dielectric metamaterials.

The insights gained from this study have potential applications in plasmonic sensors, integrated optics, and super-resolution imaging, by enabling precise control over light confinement and polarization. Furthermore, they offer promising opportunities for enhancing energy harvesting and nonlinear optical devices through tunable plasmon-polariton excitation.

References

Ahmad, Z., Oh, S.S., & Muljarov, E.A. (2024). Transverse-electric surface plasmon polaritons in periodically modulated graphene. *Physical Review Research*, 6, 023185. https://doi.org/10.1103/PhysRevResearch.6.023185.

Amiri, M., Tofigh, F., Shariati, N., Lipman, J., & Abolhasan, M. (2020). Wide-angle metamaterial absorber with highly insensitive absorption for TE and TM modes. *Scientific Reports*, 10, 13638. https://doi.org/10.1038/s41598-020-70519-8.

Carvalho, W.O.F., Oliveira, Jr O.N., & Mejía-Salazar, J.R. (2024). Magnetochiroptical nanocavities in hyperbolic metamaterials enable sensing down to the few-molecule level. *Journal of Chemical Physics, 160*(7), 071104. https://doi.org/10.1109/IPC60965.2024.10799681.

Chettiar, U.K., Kildishev, A.V., Klar, T.A., & Shalaev, V.M. (2006). Negative index metamaterial combining magnetic resonators with metal films. *Optics Express*, 14, 7872–7877. https://doi.org/10.1364/OE.14.007872.

Kanungo, T., Schilling, J. (2010). Experimental determination of the principal dielectric functions in silver nanowire metamaterials. *Applied Physics Letters*, 97, 021903. https://doi.org/10.1063/1.3462311.

Kolmychek, I.A., Pomozov, A.R., Leontiev, A.P., Napolskii, K.S., & Murzina, T.V. (2018). Magneto-optical effects in hyperbolic metamaterials. *Optics Letters*, *43*(16), 3917. https://doi.org/10.1364/OL.43.003917.

Kurilkina, S.N., Binhussain, M.A., Belyi, V.N., & Kazak, N.S. (2016). Features of hyperbolic metamaterials with extremal optical characteristics. *Journal of Optics*, *18*(8), 085102. https://doi.org/10.1088/2040-8978/18/8/085102

Lee, D., So, S., Hu, G., Kim, M., Badloe, T., Cho, H., ... & Rho, J. (2022). Hyperbolic metamaterials: fusing artificial structures to natural 2D materials. *ELight*, 2, 1-23.

Li, T., Khurgin, J.B. (2016). Hyperbolic metamaterials: beyond the effective medium theory. *Optics*, *3*(12), 1388-1396. https://doi.org/10.1364/OPTICA.3.001388.

Nguyen, P.Q.A., Nguyen, N.H. (2023). Surface plasmon-polaritons in anisotropic hyperbolic metamaterials. *Journal of Nonlinear Optical Physics & Materials*, *32*(02), 2350012. https://doi.org/10.1142/S0218863523500121.

Noginov, M.A., Barnakov, Y.A., Zhu, G., Tumkur, T., Li, H., & Narimanov, E.E. (2009). Bulk photonic metamaterial with hyperbolic dispersion. *Applied Physics Letters*, 94, 151105. https://doi.org/10.1063/1.3115145.

Novikov, V.B., Kolmychek, I.A., Pomozov, A.R., Leontiev, A.P., Napolskii, K.S., & Murzina, T.V. (2020). Magneto-optical properties of plasmonic hyperbolic metamaterials. *Journal of Physics: Conference Series*, 1461, 012120. https://doi.org/10.1088/1742-6596/1461/1/012120.

Papadakis, G.T., Yeh, P., & Atwater, H.A. (2015) Retrieval of material parameters for uniaxial metamaterials. *Physical Review B*, 91, 155406. https://doi.org/10.1103/PhysRevB.91.155406.

Rakic, A.D., Djurisic, A.B., Elazar, J.M., & Majewski, M.L. (1998). Optical properties of metallic films for vertical-cavity optoelectronic devices. *Applied Optics*, 37, 5271-5283. https://doi.org/10.1364/AO.37.005271.

Shekhar, P., Atkinson, J., & Jacob, Z. (2014). Hyperbolic metamaterials: fundamentals and applications. *Nano Convergence*, *19*(1), 14-1–14-17. https://doi.org/10.1186/s40580-014-0014-6.

Simmons, J.H., Potter, K. S. (2000). *Optical Materials*. Academic Press.

Slobozhanyuk, A.P., Ginzburg, P., Powell, D.A., Iorsh, I., Shalin, A.S., Segovia, P., ... & Zayats, A.V. (2015). Purcell effect in hyperbolic metamaterial resonators. *Physical Review B, 92*(19), 195127. https://doi.org/10.1103/PhysRevB.92.195127.

Song, J., Cheng, Q., Lu, L., Li, B., Zhou, K., Zhang, B., Luo, Z., & Zhou, X. (2020). Magnetically Tunable Near-Field Radiative Heat Transfer in Hyperbolic Metamaterials. *Physical Review Applied*, 13, 024054. https://doi.org/10.1103/PhysRevApplied.13.024054.

Sun, J., Litchinitser, N.M., Zhou, J. (2014). Indefinite by Nature: From Ultraviolet to Terahertz. *ACS Photonics*, 1, 293–303. https://doi.org/10.1021/ph4000983.

Sun, Z., Zuo, X., Guan, T., & Chen, W. (2014). Artificial TE-mode surface waves at metal surfaces mimicking surface plasmons. *Optics Express*, *22*(4), 4714-4722. https://doi.org/10.1364/OE.22.004714.

Wang, H., Wang, T., Yan, R., Yue, X., Wang, L., Wang, Y., ... & Wang, J. (2022). Coupling plasmon-waveguide resonance and multiple plasma modes in hyperbolic metamaterials for high-performance sensing. *Nanotechnology, 33*(46), 465203. https://doi.org/10.1088/1361-6528/ac86dd.

Wang, S., Zhao, C., & Li, X. (2019). Dynamical Manipulation of Surface Plasmon Polaritons. *Applied Sciences*, *9*(16), 3297. https://doi.org/10.3390/app9163297.

Wurtz, G.A., Pollard, R., Hendren, W., Wiederrecht, G.P., Gosztola, D.J., Podolskiy, V.A., & Zayats, A.V. (2011). Designed Ultrafast Optical Nonlinearity in a Plasmonic Nanorod Metamaterial Enhanced by Nonlocality. *Nature Nanotechnology*, 6, 107–111. https://doi.org/10.1038/nnano.2010.278.

Zayats, A.V., Smolyaninov, I.I., & Maradudin, A.A. (2005). Nano-optics of surface plasmon polaritons. *Physics Reports*, *408*(3–4), 131-314. https://doi.org/10.1016/j.physrep.2004.11.001.